




Enhanced thermoregulation performance of knitted fabrics using phase change material incorporated thermoplastic polyurethane and cellulose acetate nanofibers

Çiğdem Akduman¹  | Nida Oğlakcıoğlu²  | Ahmet Çay² 

¹Department of Textile Technology, Denizli Vocational School of Technical Sciences, Pamukkale University, Denizli, Turkey

²Department of Textile Engineering, Faculty of Engineering, Ege University, Izmir, Turkey

Correspondence

Nida Oğlakcıoğlu, Department of Textile Engineering, Faculty of Engineering, Ege University, Bornova, Izmir, Turkey.
Email: nida.gulsevin@ege.edu.tr

Funding information

Pamukkale University Research Foundation, Grant/Award Number: 2022HZDP010

Abstract

Nanofibers act as carriers in systems containing functional materials produced via electrospinning method. By this way, it is possible to transport functional materials with polymer nanofibers, besides having a large surface area compared to their volume, the encapsulation process, which includes complex preparation processes, is eliminated here, and functional materials such as phase-change materials (PCMs) can be conveniently integrated directly into the carrier material by electrospinning method. The resulting nanofiber membrane can also be used in combination with textile fabrics. This study aims to develop PCM containing nanofibrous membrane coated knitted fabric structures with heat regulation capabilities. Two types of PCMs, hexadecane and octadecane loaded into thermoplastic polyurethane (TPU) and cellulose acetate (CA) nanofibers, directly electrospun on cotton (CO), cotton/polyester (CO/PES), cotton/acrylic (CO/PAC) knitted fabrics for thermoregulation. These nanofiber-coated fabrics were characterized by scanning electron microscopy (SEM) and differential scanning calorimetry (DSC), and their comfort properties were evaluated by water vapor and air permeability tests and compared with a commercial microcapsule impregnated fabric. According to DSC results, PCM incorporated CA nanofibers had better heat storage capacity than TPU nanofibers and microcapsule applied fabrics. Although PCM-loaded CA nanofibers may not block airflow as effectively as TPU nanofibers, when a proper coating is achieved air permeability can be decreased to 21.70 L/m²/s, along with a heat storage capacity of 26.38 J/g and still having permeability to water vapor (%40).

Highlights

- Phase change materials were integrated directly to the carrier material by electrospinning
- PCM integrated nanofiber coating reduced air permeability
- PCM integrated nanofiber coating did not block water vapor permeability
- Electrospun cellulose acetate +PCM coating had better heat storage capacity

KEYWORDS

electrospinning, nanofiber, permeability, phase change material, textile fabric, thermal regulation

1 | INTRODUCTION

Textiles have been a part of our lives since the early days of human existence, emerging from the need to protect oneself from cold, heat, and other natural elements. Initially, they were used solely for protection and covering. However, they later evolved to serve many functionalities, one of which is thermal regulation to improve the clothing comfort of the wearer. For this purpose, garments and household textiles can be manufactured by incorporating phase change material (PCM) microcapsules. PCMs can be used as thermal storage and control materials due to the heat absorption and release during phase transitions between solid–solid and solid–liquid phases within a narrow temperature range.^{1–3} Among many organic and inorganic PCMs, microencapsulated paraffins are particularly preferred for textiles,⁴ and this phase change technology is applied by incorporating PCM microcapsules into textile structures. PCM microcapsules are produced with a PCM core that can change its physical state in both directions within the specified temperature range, along with a polymer shell.⁵ The protective microcapsule shell ensures that the PCM remains at the site of application in its liquid form.^{6,7} PCM microcapsules can be applied to fabrics by embedding them into acrylic fibers, polyurethane foams, or through a coating application. PCM technologies can also be applied in protective clothing for challenging environments, ranging from cold water to hot deserts.

In cold environments, the primary purpose of clothing is to protect the wearer from cold and prevent a significant drop in skin temperature. Conversely, when it is hot, PCMs melt and absorb the external heat, keeping the body relatively cool. When PCMs reach their melting point (T_m) and/or crystallization temperature (T_c), or when they exceed or fall below these temperatures, they can absorb or release heat, respectively, from/to the surroundings in dynamic heat exchange processes, resulting in thermal regulation. Thus, applying these PCMs to garments creates a relatively comfortable microclimate.⁷

More than 500 different PCMs were described in the PCMs Handbook published by NASA in 1971.⁸ The most common PCMs in textiles are paraffin waxes with various phase change temperatures (melting and crystallization) depending on their carbon numbers. The properties of some of these phase change materials are encapsulated in microcapsules ranging from 1 to 30 μm in diameter.⁹ PCM

integrated fibrous materials can be produced by melt spinning, direct application of PCMs or PCM nano/microcapsules into the fabric, or fiber as well as electrospinning.³

Traditional insulation relies on the air trapped within garment layers and garment should show enough resistance to airflow. In windy conditions, porous structures let the air inside, and thermal insulation decreases significantly. Situations such as garment wetting or perspiration condensation inside the clothing similarly affect thermal comfort. The use of interactive insulation systems involving PCMs can enhance thermal comfort. Coating a PCM-containing nanofibrous layer is an innovative method compared to traditional microcapsule technology. The incorporation of a PCM-containing nanofibrous layer into traditional fabrics will increase the potential use of these fabrics as outerwear, as they exhibit both water-repellent and air-impermeable barrier effects.

Van Do et al.¹⁰ produced core/sheath nanofibers using polyethylene glycol (PEG)/polyvinylidene fluoride (PVDF) via coaxial electrospinning. PEG was utilized as the PCM. They determined the thermal properties of the nanofibers prepared using different molecular weight PEGs through DSC analyses. Paroutoglou et al.¹¹ fabricated PCM microfibers using a coaxial electrospinning method with polycaprolactone (PCL) solutions of 9% w/v and 12% w/v in dichloromethane as the shell material. Sodium dodecyl sulfate and 10% w/v Polyvinyl alcohol were emulsified with PCM to form the core of the fibers. The thermal behavior of PCM, PCM emulsions, and fibers produced by electrospinning was analyzed using differential scanning calorimetry (DSC). In their study, Haghghat et al.¹² selected polyvinylpyrrolidone (PVP), polyvinylidene fluoride (PVDF), and polyacrylonitrile (PAN) polymers as shell materials and n-octadecane as the PCM material for low-temperature PCM. Their thermoregulation properties were determined using DSC analyses and a simulated body system. Salimian et al. developed PVA/PEG/TiO₂/Ag PCM fibrous nanocomposites for thermal energy management and storage applications. Thermal performances of the PCM-integrated fibrous composites were evaluated with respect to different amounts of AgNO₃ and TiO₂ and PVA to PEG ratios.¹³

Nanofiber surfaces, due to their high porosity and very low thickness, do not negatively impact comfort properties when transferred to fabric surfaces and do not

increase fabric weight. The combination of PCMs with nanofibers to create a membrane and their integration with different fabric structures can lead to the development of various structures such as thin-thick, woven-knitted, single layer-double layer, and more. These fabrics will possess thermoregulation properties, remain lightweight, allow breathability due to their nano- to microporous structure permitting moisture passage, and enhance comfort levels in cold environments with their water and air-impermeable structures.

This study aims to develop nanofibrous membranes containing PCM coated knitted fabric structures with heat regulation capabilities. For this scope, thermoplastic polyurethane (TPU) and cellulose acetate (CA) were selected as carrier polymers, and hexadecane and octadecane, as PCMs. TPU was chosen because of its high mechanical properties and easy electrospinnability.¹⁴ Its nontoxicity, toughness and functionality have led to the widespread use of TPU. CA is a derivative of a naturally occurring raw material and is an alternative to synthetic polymers produced from petroleum.¹⁵ CA nanofibers could be utilized for various applications ranging from affinity membranes¹⁶ to tissue engineering^{17,18} and sensors.¹⁹ CA was chosen because CA nanofibers form a relatively bulkier layer than TPU nanofibers. CA is also stable in water and has good solubility in organic solvents.^{20,21} To the best of the authors' knowledge, hexadecane and octadecane PCM materials were directly loaded into the TPU and CA polymer solutions without core-shell spinning and PCM loaded nanofibers were produced by traditional electrospinning method onto knitted jersey fabrics for the first time. The produced nanofibers were collected onto cotton (CO), cotton/polyester (CO/PES) and cotton/acrylic (CO/PAC) single jersey fabrics to determine whether fiber type has a significant effect on thermal regulation properties. These nanofiber-coated fabrics were characterized, and their properties were compared with a commercial microcapsule impregnated fabric. Nanofibrous surfaces are defined as breathable surfaces due to their high porosity, which allows high water vapor transmission. The integration of phase change materials with nanofibrous membranes aims to develop innovative smart textiles that are both breathable and capable of managing heat.

2 | MATERIALS AND METHODS

2.1 | Materials

The TPU (Pellethane 2103-80AE) was provided from Velox (Lubrizol Advanced Materials). CA with an average molecular weight of $\sim 30,000$ g/mol and acetylation

degree of 39.8 wt.%, acetone, dimethylacetamide (DMAc), N,N dimethylformamide (DMF) and chloroform were supplied from Sigma Aldrich Chemical Company. The PCMs, n-octadecane and n-hexadecane were purchased from BostonChem through DAF Limited Company. Their properties were given in Table 1. PCM microcapsule Rucotherm EPV (solid content about 35%–40%) and its binder RUCO-PLAST PMN were supplied by the Rudolf GmbH Turkey. Three types of single jersey knitted fabrics produced by using Ne 30/1 yarns containing 100% CO, 50/50% CO/PES and 50/50% CO/PAC were supplied from supplied from NESA Tekstil. The weight of each fabric was about 155 ± 5 g/m².

2.2 | Impregnation of PCM microcapsules

Three concentrations of 100, 150, and 200 g/L Rucotherm EPV PCM microcapsule solutions including 30, 40, and 50 g/L Ruco-Plast PMN binder, respectively, at pH 5.5 were prepared for impregnation. Concentrations were adjusted according to product specs. Each type of fabric (CO, CO/PES, and CO/PAC) were impregnated in a laboratory scale padder at 70% pick up ratio, then dried for 3 min at 110°C, and finally heat treated for 1 min at 160°C in an oven. Fabrics were coded with microcapsule concentrations of 100, 150, and 200, microcapsule abbreviations, and fabric types. For example, the sample 100EPV-CO stands for 100 g/L microcapsule solution was impregnated onto CO knitted fabric.

TABLE 1 Properties of used PCMs.

PCM	Properties
Hexadecane	BOSTONCHEM BHM-810866- 500ML (N-hexadecane, AR, 98%) CAS Number: 544–76- 3 Formula: C ₁₆ H ₃₄ Molecular Weight: 226.44 g/mol Melting Enthalpy: 182.6 J/g* Melting Temperature: 18.2°C** Crystallization Temperature: 16.2°C*
Octadecane	BOSTONCHEM BOM-815232-100G (octadecane, 99%) CAS Number: 593–45- 3 Formula: C ₁₈ H ₃₈ Molecular Weight: 254.49 g/mol Melting Enthalpy: 236.6 J/g* Melting Temperature: 28.2** Crystallization Temperature: 25.4°C*

*Mondal, 2008.²²

**Mäkinen et. al, 2006.⁹

2.3 | Electrospinning of PCM incorporated nanofibers

Neat TPU solution was prepared by dissolving TPU granules in the concentration of %9 (w/w) in DMF at room temperature. The solution was stirred with a magnetic stirrer for 12 h. For the preparation of PCM-loaded TPU solutions, first PCMs were dissolved in chloroform. For each 20 g PCM/TPU solution, 3 g chloroform was used to dissolve PCMs. Then, TPU solution was added to this PCM solution to achieve a final 9% w/w TPU solution and stirred at 40°C. 20, 30, and 40% of hexadecane and octadecane were added over the TPU weight for PCM-loaded TPU solutions.

CA solution was prepared by dissolving CA powder in the concentration of 16% w/v in acetone/DMAc in the volume ratio of 2:1 at 50°C and stirring for 3 h. For the preparation of PCM/CA solutions, the 16% (w/v) CA solution was directly added to the weighed amount of 20, 30, and 40% of hexadecane and octadecane over the CA weight and stirred for a further 2 h with a magnetic stirrer at 40°C.

Electrospinning of the polymer solutions was carried out by a set-up consisting of a single flat-tip stainless steel needle, a grounded rotating metal drum collector, and a high-voltage supply. TPU and CA solutions were electrospun at voltages of 13 and 15 kV and tip-to-collector distances of 18 and 15 cm, respectively. Feeding rates of 0.4–0.5 mL/h were used for all solutions. Each solution (neat and PCM incorporated CA and TPU solutions) was electrospun for 5 h onto CO, CO/PES, and CO/PAC single jersey fabrics. Fabrics were coded with their PCM concentrations of 20%, 30%, and 40%, PCM abbreviations of “Oc” for octadecane, “Hex” for hexadecane, polymer names of TPU and CA, and the fabric types of CO, CO/PES, and CO/PAC. For example, 20% Oc TPU-CO/PES sample stands for TPU nanofibers including 20% of octadecane were electrospun onto CO/PES knitted fabric.

2.4 | Tests and characterization

The morphologies of neat and PCM-loaded TPU and CA nanofibers and PCM microcapsule-impregnated fabrics were characterized using scanning electron microscopy (SEM, Phenom G2pro). Each sample was sputtered by a Quorum Q150R S ion sputtering device with a thin layer of gold with 20 mA, 10^{-1} mBar prior to SEM observation. The mean diameter of the nanofibers from 50 measurements was calculated from the SEM images by using the Image J program.

The thermal behavior of neat and PCM-incorporated nanofibers and microcapsule applied fabrics was

investigated by differential scanning calorimetry (DSC) (TA Instrument, Q20). Samples were sealed in an alumina pan and heated under a continuous nitrogen purge at the rate of 50 mL/min from -20 to 100°C at a heating rate of $5^\circ\text{C}/\text{min}$.

Thermogravimetric analysis of selected nanofibers was investigated by TGA (PERKIN ELMER TGA-4000) by heating samples from 25 to 600°C at a rate of $10^\circ\text{C}/\text{min}$ under a continuous nitrogen purge at a rate of 20 mL/min.

The weight and thickness of the nanofiber-coated samples were reported according to EN 12127:1997 and EN ISO 5084:1996, respectively.

The water contact angle (WCA) was measured by using a CAM 200 contact angle meter (KSV Instruments, Helsinki, Finland). The contact angles with distilled water were measured on the upper surface of the blank fabrics and nanofiber surfaces. The measurements were conducted room temperature (25°C) and at a relative humidity of 40–50%. A droplet of water with a volume of 2 μL was deposited onto the surface from 5 cm by vibrating the tip of a micro-syringe. A real-time camera captured the image of the droplet. The droplet was recorded on the membrane surface after 1 s.

For thermal camera evaluation, the samples were placed on a heated plate, which was kept at a constant surface temperature of 34°C , and thermal images were taken every 10 s using a thermal camera (Testo 875-1i). The average surface temperature was calculated from the images and evaluated (Figure 1).

Water vapor permeability measurements were carried out of Permetest (Sensora Company, Liberec, Czech Republic) in accordance with ISO 11092. The instrument works according to the principle of heat flux sensing. The temperature of the measuring head is kept at room temperature for isothermal conditions. Some heat is lost after the water flows into the measuring head. This instrument measures the heat loss from the measuring head due to the evaporation of water in bare state (without a sample) and covered with sample.^{23,24}

Relative water vapor permeability of the textile sample (P_{wv} , %) is determined from Equation (1), where U_s is the heat loss of the free wet surface without a sample and U_o is the heat loss of the wet measuring head with the sample.²⁵

$$P_{\text{wv}} = 100 U_s / U_o \quad (1)$$

Air permeability measurement was carried out according to EN ISO 9237 with FX3300 air permeability tester (Textest, Switzerland). 5 cm² measurement area and 100 Pa pressure drop were used for the measurement. It is the rate of airflow passing through a known area under a prescribed air pressure differential between

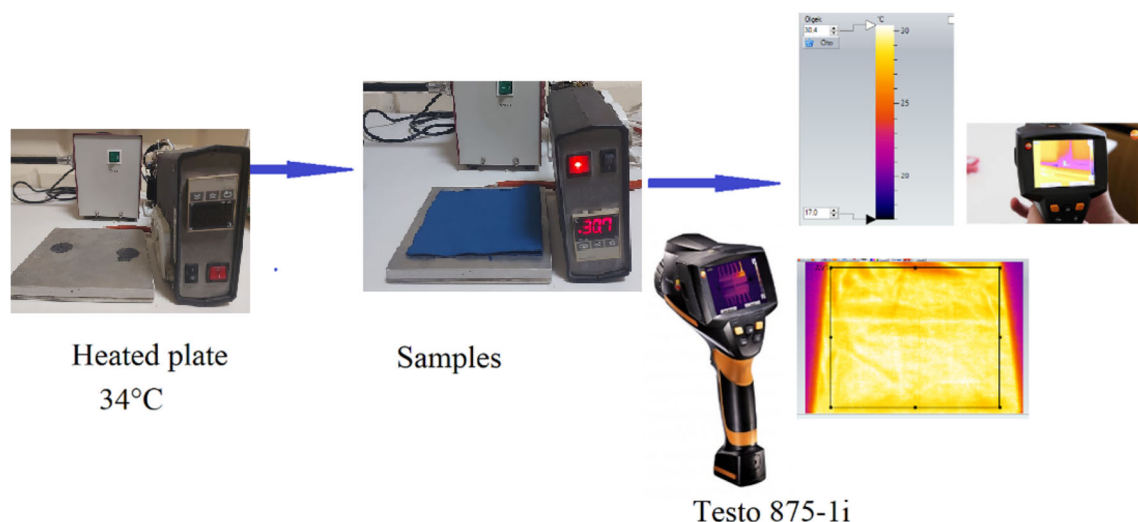


FIGURE 1 Illustration of thermal camera evaluation.

the two surfaces.²⁶ The air is drawn through the specimen into a closed chamber and out through an orifice that measures the flow.

3 | RESULTS AND DISCUSSIONS

3.1 | Morphology

In the first part of the study, microcapsules were applied to CO, CO/PES, and CO/PAC single jersey fabrics by impregnation at three concentrations of 100, 150, and 200 g/L, and fixation processes were completed. SEM images of 200 g/L applied CO, CO/PES, and CO/PAC were given in Figure 2. Microcapsules and binder attachments could be observed in the SEM images.

In the second part, electrospinning trials were carried out for direct encapsulation of PCMs into nanofibers. The crystallization temperature of the selected hexadecane is 16.2°C, while the crystallization temperature of octadecane is 25.4°C. Although the spinning solutions were prepared by heating (40°C), during spinning process conducted at $23 \pm 2^\circ\text{C}$ in the laboratory environment, due to the cooling of the solutions, they crystallized inside the syringe, causing spinning to stop. To remove the crystallization, the syringe was heated, and spinning continued for 5 h to complete. More crystallization problems were encountered in the electrospinning solutions loaded with octadecane due to its higher crystallization temperature. It was observed that the addition of PCMs into the spinning solution reduced the electrospinnability of the CA nanofibers and disrupted the nanofiber structure. The CA nanofibers loaded with hexadecane were completed by heating. Due to the continuous crystallization problem of

the solution studies with CA loaded with octadecane were canceled. Also, despite heating, nanofiber production could not be obtained with CA polymer loaded with hexadecane as shown in Figure 3. Since CA solutions were directly added onto hexadecane, it was not possible to dissolve hexadecane and obtain a processable electrospinning solution. However, it was seen that, hexadecane was present on the produced surface and could still be used as a PCM coating material.

All produced nanofibers were white and their SEM images of Oc TPU and Hex TPU nanofibers were given in Figures 4 and 5, respectively. It was observed that 40% Oc TPU nanofibers were thicker, and less uniform compared to 30% Oc TPU and 20% Oc TPU nanofibers.

Since same PCM loaded electrospinning solutions were used for each fabric, SEM images of nanofibers on the CO jerseys were given in the figures. However, it was seen that, some other SEM images of Oc TPU nanofibers on CO/PES were also not as smooth as Figure 3A–D. It was obvious that octadecane loaded electrospinning solutions should be spun at a temperature above melting point of octadecane for better and consistent nanofiber morphology. Mean fiber diameter of 20%Oc TPU and 30%Oc TPU nanofibers were about 549 ± 161 and 478 ± 110 nm. However, loading 40%Oc made the electrospinning difficult and caused clogging which resulted in unsuccessful nanofiber production and membrane like fused surface. When compared to Oc TPU nanofibers, morphology of the Hex-TPU nanofibers were better and smoother. Mean diameters of 20, 30, and 40% Hex TPU nanofibers were 749 ± 215 , 803 ± 249 , and 680 ± 192 nm. Statistically, when compared with One-Way ANOVA, there was not any significant difference between the mean nanofiber diameters ($p > 0.05$).

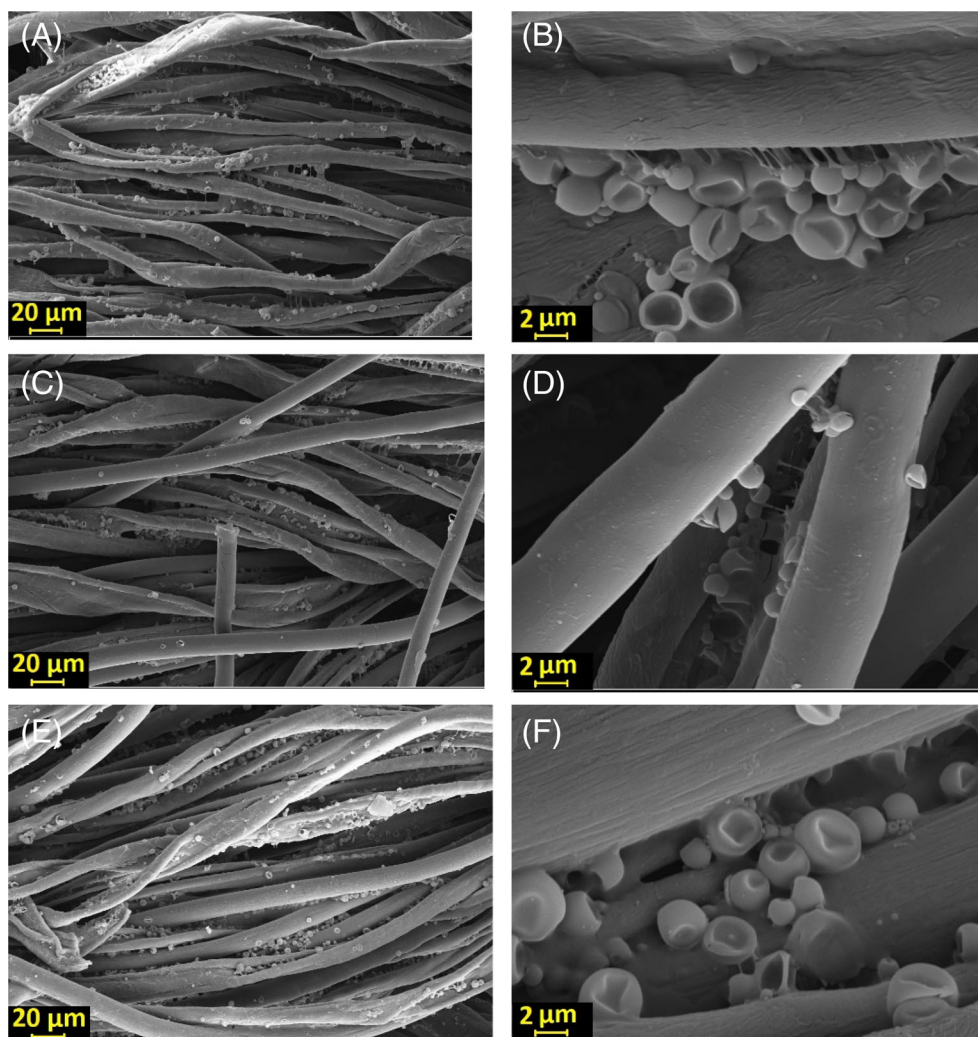


FIGURE 2 SEM images of 1000 and 10,000x magnifications of (A) and (B) 200EPV-CO, (C) and (D) 200EPV-CO/PES, and (E) and (F) 200 EPV-CO/PAC, respectively.

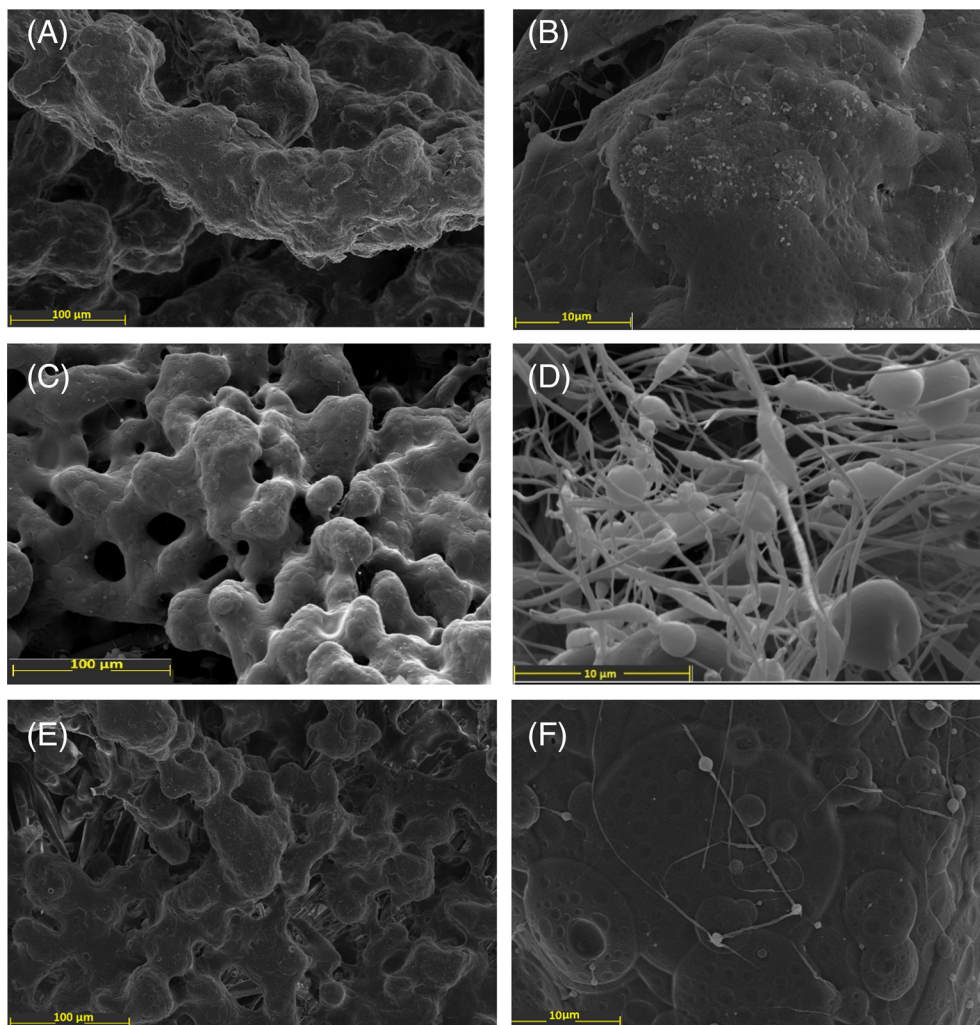
3.2 | DSC results

DSC spectra for microcapsule-applied fabrics and PCM-loaded nanofibers were given in Figure 6. DSC studies were conducted between -20 and 100°C , and since there would be no glass transition and melting in the fabric structures of CO, CO/PES, and CO/PAC within this temperature range, DSC curves were provided independently from the fabric type. From the DSC curves of microcapsules applied fabrics, 100 EPV did not show any heat flow, besides, 0.2344 and 0.5258 J/g of heat flows were recorded at melting of 17°C for 150 EPV and 200 EPV microcapsule loadings, respectively (Figure 6A). Since these microcapsules were applied with a significant amount of binder, its glass transition could also be seen between ~ 50 to 90°C . From these results, it can be concluded that a very low heat flow was observed for EPV microcapsule applications. Cetiner and Belten²⁷ used Mikrathermic P-P and Mikrathermic P-P as microcapsules and achieved melting enthalpy of 2.70 and 1.62 J/g, respectively. Shin et al.¹ used melamine-formaldehyde

microcapsules containing eicosane, and they were able to achieve a maximum of 4.44 J/g of melting enthalpy with a 22.9% add-on of microcapsules. Nejman et al.⁵ applied n-octadecane including microcapsules by printing, coating, and padding technique, and melting enthalpies were reported to be 36.5 , 23.4 , and 13.4 J/g, respectively. When compared to our results, their relatively higher results were related to the much higher applied amount of the microcapsules (20 wt.%). Based on our results and literature reviews, it was observed that significantly high heat storage capacities cannot be achieved with microcapsule applications. In our study, due to the relatively thin knitted jersey fabrics and low add-on, it was more difficult to achieve high melting enthalpy. Therefore, it is necessary to increase the amount of microcapsule application for better thermoregulation; this can be achieved by applying more microcapsules to a higher-weight fabric or a filling material with higher weight.

The DSC curves of 20, 30 and 40% Oc TPU nanofibers were given in Figure 6B. In the DSC curves of 30 and 40% Oc TPU nanofibers, heat flow of 1.618 and 4.914 J/g,

FIGURE 3 SEM images of 1000 and 10,000x magnifications of (A) and (B) 20% Hex CA-CO, (C) and (D) 30% Hex CA-CO, and (E) and (F) 40% Hex CA-CO, respectively.



respectively, were observed at 28°C. Melting point of octadecane slightly shifted to 28°C due to being inside the TPU nanofibers. However, the loaded octadecane amount remained low in the 20% Oc TPU nanofibers showing no heat storage capability. 30 and 40% Oc TPU nanofibers showed also very low heat flow of 1.618 and 4.914 J/g, respectively, but higher when compared to microcapsules.

In Figure 6C, the DSC curves of HexTPU nanofibers were presented. The melting point of hexadecane was not observed in these curves, and it was observed that Hex TPU nanofibers did not exhibit heat storage capability. This was thought to be due to the ineffective dissolution of hexadecane in the TPU solution and its inability to be processed into nanofibers via electrospinning. In Figure 6D DSC curves of Hex CA nanofibers were shown. Melting of hexadecane was observed at 19–20°C on all three DSC curves. The heat flow in Hex CA samples was 1.884, 3.857, and 26.38 J/g, respectively. The heat storage capability of 40% Hex CA samples was higher than that of all other produced samples. According to these results,

although successful electrospinning of CA nanofibers loaded with hexadecane could not be achieved, hexadecane was incorporated into the membrane-like coating by electrospinning rather than electrospinning, resulting in relatively high heat capacity.

McCann et al.²⁸ were used melt electrospinning for producing hexadecane, octadecane and eicosane loaded TiO₂-polyvinylpyrrolidone (PVP) nanofibers as core-shell. They achieved 71 J/g of melting enthalpy corresponding to a 31% wt. loading of hexadecane, 114 J/g, corresponding to a loading of 45% wt. octadecane and 88 J/g, corresponding to 36% wt. loading of eicosane. When we compare these results with our results, melt spinning seems to be more convenient for producing PCM loaded nanofibers. Van Do et al.¹⁰ also fabricated Polyethylene-glycol (PEG)/polyvinylidene fluoride (PVDF) core/shell nanofibers by conventional electrospinning. They had the largest content of PEG in the core up to 42.5 wt% with a latent heat of 68 J/g. Wang et al.²⁹ selected hexadecane and eicosane as PCM materials. They measured 11.5 J/g for the hexadecane, and 11.8 J/g for the

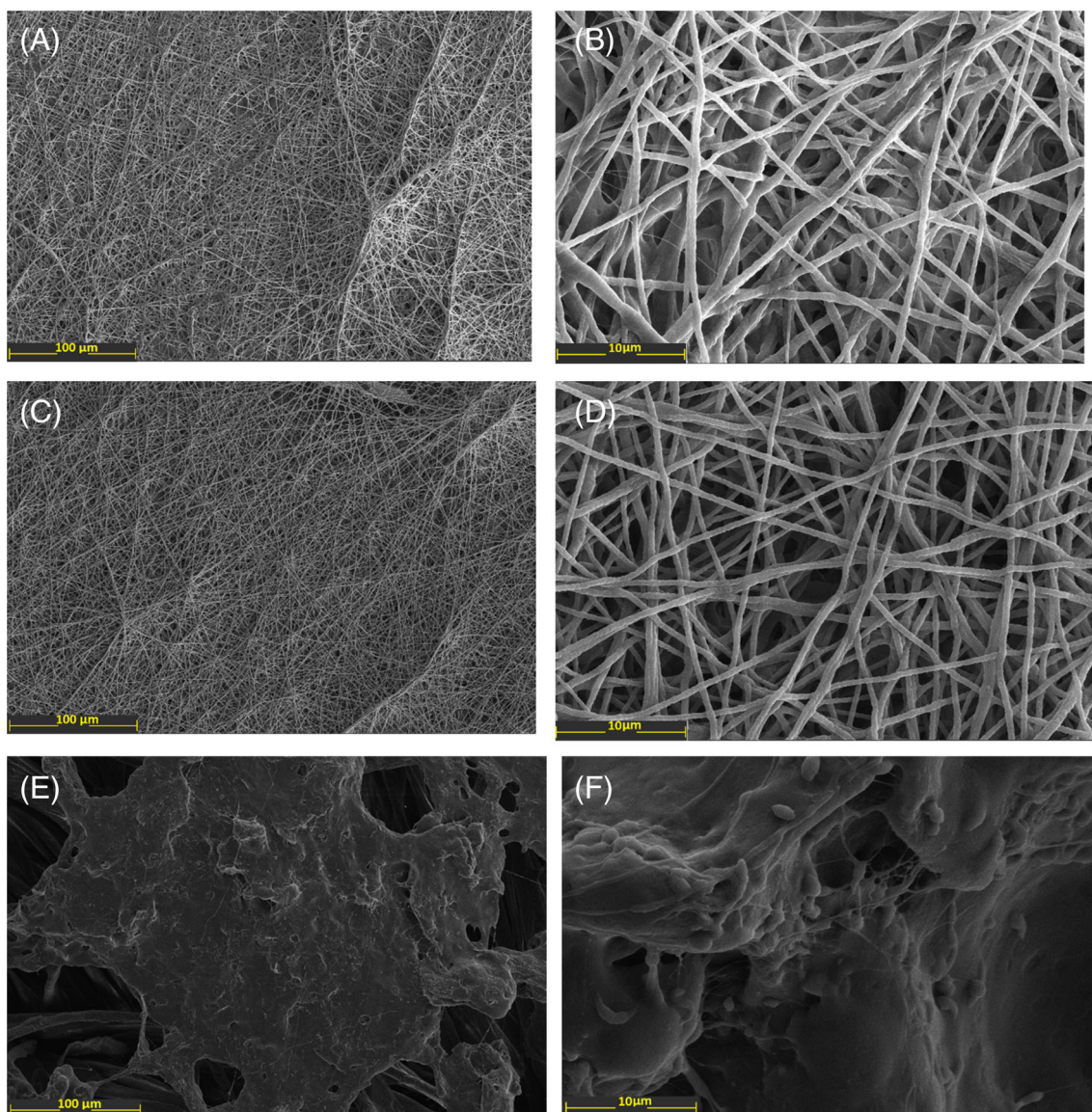


FIGURE 4 SEM images of 1000 and 10,000x magnifications of (A) and (B) 20% Oc TPU-CO, (C) and (D) 30% Oc TPU-CO, and (E) and (F) 40% Oc TPU-CO, respectively.

eicosane loaded PVP core/shell nanofibers. Sun et al.³⁰ produced a core-shell fiber containing n-octadecane as the core and polyvinyl butyral (PVB) as shell material and achieved melting enthalpy of 105.9 J/g. Haghighat et al.¹² recently investigated PVP, PVDF and polyacrylonitrile (PAN) as shell materials, n-Octadecane as core PCM material. They were able to achieve enthalpy of about 80 J/g for PCM-PVP. When we compare these results with the present study, core-shell electrospinning appears to be more effective for PCM loading to the nanofibers due to the significantly higher melting enthalpy results. However, it should be noted that the processing of core-shell electrospinning is much more complicated and requires special equipment such as needle-in-needle assemblies and extra feeding pump for each solution. On the other hand, direct loading of PCMs

through classical electrospinning or electrospaying is much easier and therefore it could be taken as a practical alternative option. Melting enthalpy, and therefore heat storage capacity, could be increased by increasing the amount of PCM and spinning in a heated environment.

3.3 | TGA results

TGA curves of 40%Hex TPU, TPU, 40%Hex CA, and CA nanofibers were given in Figure S1. For TPU and 40%Hex TPU nanofibers, thermal degradation started at approximately 270°C, while it ceased at approximately 470°C. They lost half of their mass at 385°C, leaving merely ~6% residue at 600°C. Both neat CA and 40%Hex CA nanofibers lost about 6% mass at temperatures up to 95°C due

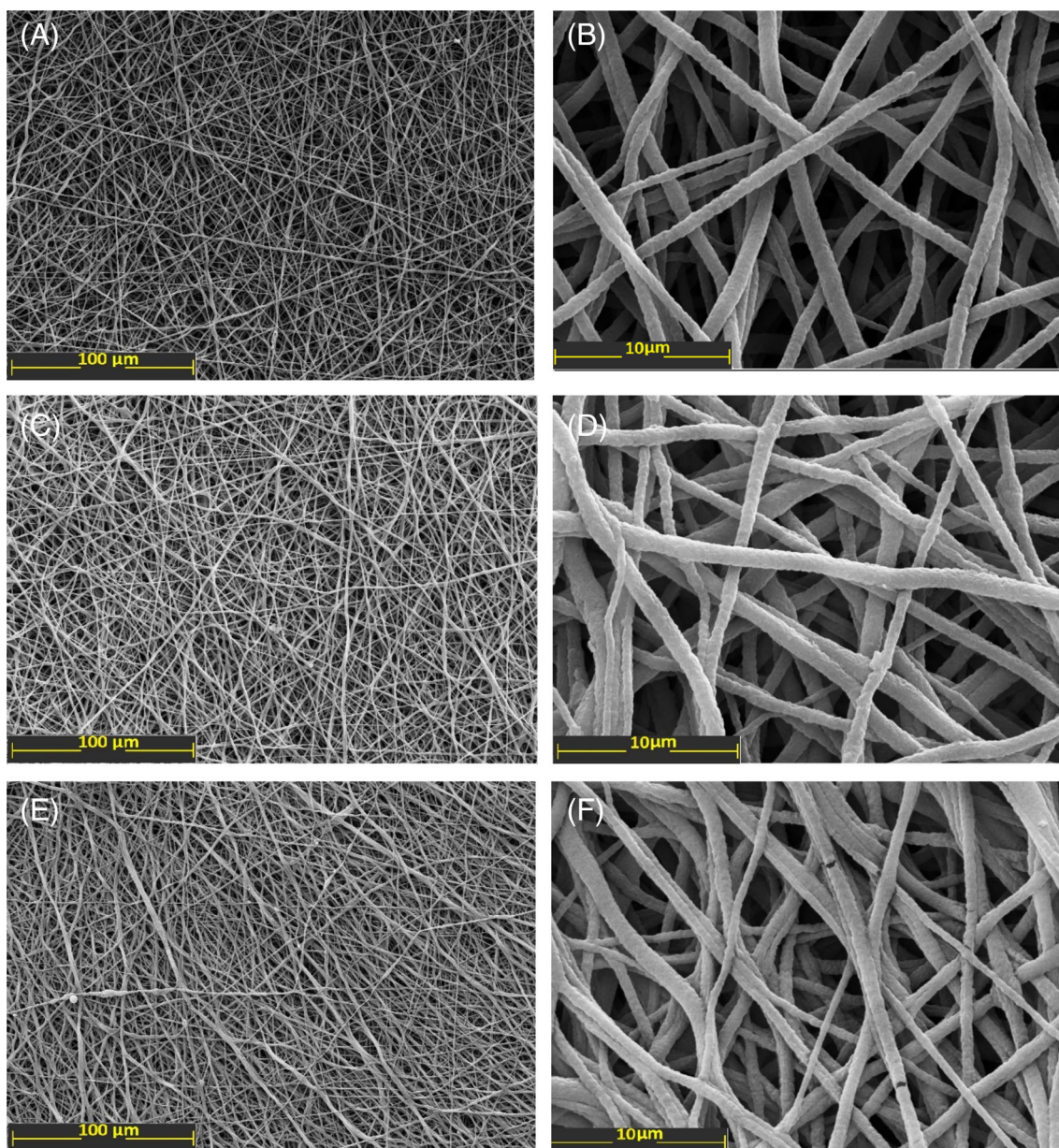


FIGURE 5 SEM images of 1000 and 10,000x magnifications of (A) and (B) 20% Hex TPU-CO, (C) and (D) 30% Hex TPU-CO, and (E) and (F) 40% Hex TPU-CO, respectively.

to the evaporation of absorbed moisture. The decomposition of CA and 40%Hex CA began around 280°C and lost half of its mass at 360°C, leaving merely ~10% residue at 600°C. It was indicated that PCM incorporation did not affect the thermal degradation of TPU and CA nanofibers (Figure 7).

3.4 | Weight and thickness results

Weight and thickness measurements of Hex CA and Hex TPU fabrics weight and thickness measurements were also carried out and reported in Table 2. 40%Hex TPU nanofiber coating weighed approximately 20–30 g/m²,

relatively causing a thin layer with a thickness between 0.58 and 0.64 mm. Since TPU coating had some elasticity due to the TPU structure, Hex TPU nanofiber coating did not affect the handle of these fabrics. 40%Hex CA coating approximately weighed 50 g/m² on the CO and CO/PES fabric and form a thicker layer because of the CA nanofibers with thickness between 0.80 to 0.84 mm. Only the 40% Hex CA CO/PAC sample had a thick (1.09 mm) and heavy coating due to very uneven spinning. Possibly, the formation of more splashes rather than nanofibers caused this inconsistent coating. When compared to Hex TPU nanofiber coatings, Hex CA nanofibers were thicker and heavier thus their handle was slightly tougher.

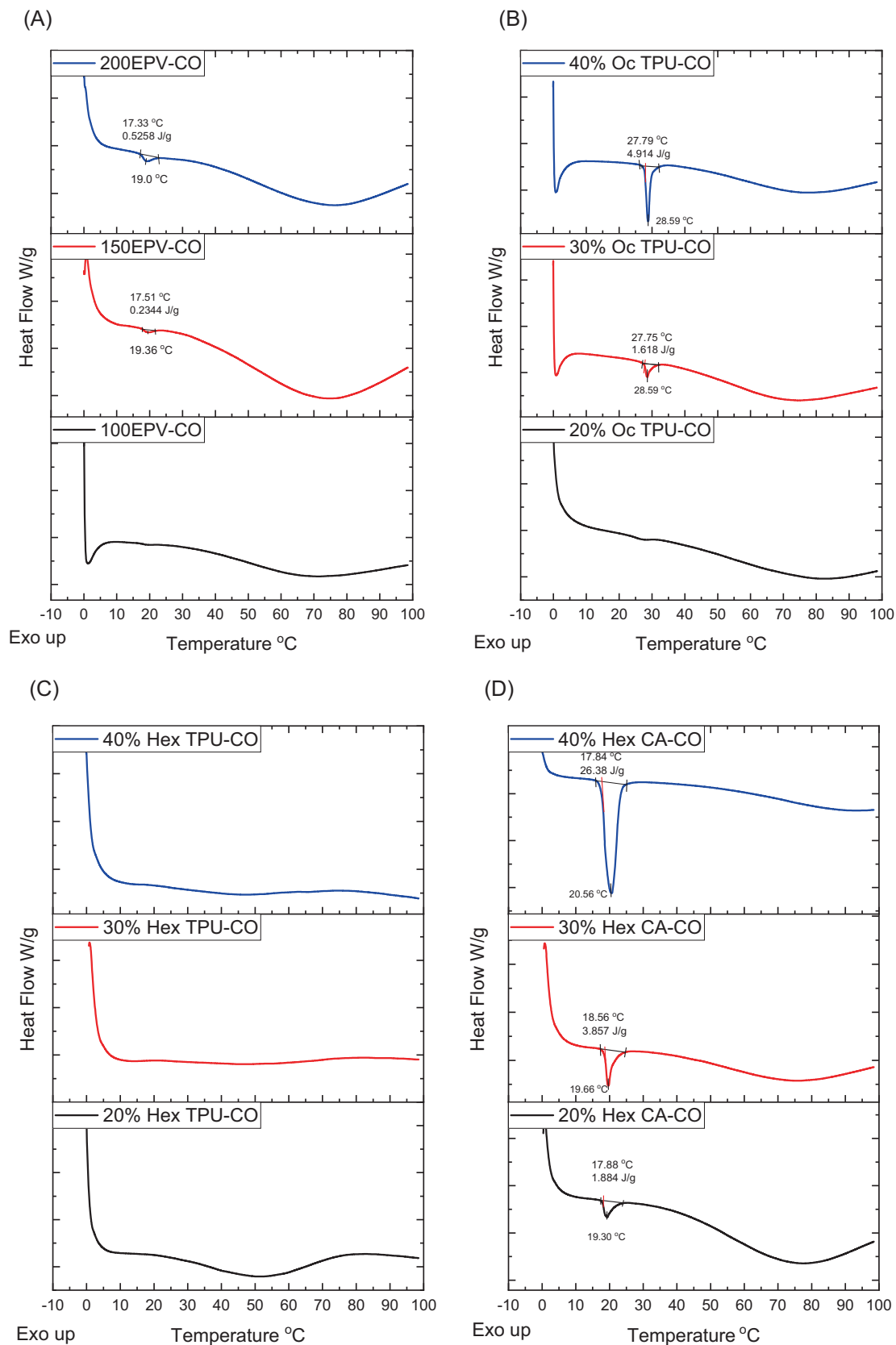


FIGURE 6 DSC spectra of microcapsule applied (A); 100, 150, and 200EPV-CO, nanofibers; (B) 20, 30, and 40%Oc TPU-CO, (C) 20, 30, and 40% Hex TPU-CO, and (D) 20, 30, and 40% Hex CA-CO samples.

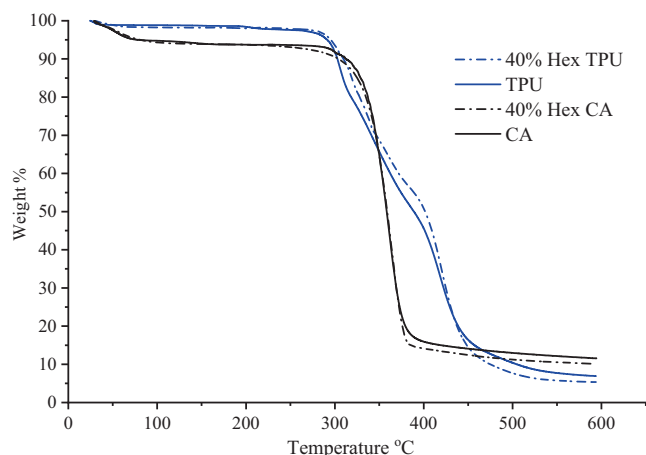


FIGURE 7 TGA curves of 40%Hex TPU, TPU, 40%Hex CA, and CA nanofibers.

TABLE 2 Weight and thickness of CO, CO/PES, CO/PAC and 40%Hex TPU and CA coated CO, CO/PES, CO/PAC fabrics.

Sample	Weight (g/m ²)	Thickness (mm)
CO	160.6	0.59
CO/PES	166.7	0.48
CO/PAC	150.0	0.57
40%Hex TPU-CO	180.8	0.61
40%Hex TPU-CO/PES	195.8	0.58
40%Hex TPU-CO/PAC	172.9	0.64
40%Hex CA-CO	210.8	0.84
40%Hex CA-CO/PES	220.5	0.80
40%Hex CA-CO/PAC	261.1	1.09

TABLE 3 WCAs and droplet images of CO, CO/PES, CO/PAC and 40%Hex TPU and CA coated CO, CO/PES, CO/PAC fabrics.



3.5 | WCA results

WCA values between water droplets and the samples were measured and images were taken after 1 s. The average WCA(°) values of the right, middle, and left were reported in Table 3 with the droplet images. CO, CO/PES, and CO/PAC base fabric were all hydrophilic. WCAs of all samples were almost under 90° which indicated that they were not hydrophobic. After 15 s, 40%Hex TPU-CO, 40%Hex TPU-CO/PAC, 40%Hex CA-CO, and 40%Hex CA-CO/PAC samples mostly kept their WCAs, and other samples absorbed the water completely and the final WCAs were 0°. This might be the PCM's existence on the surfaces; however, they were still considered not hydrophobic.

3.6 | Thermal imaging results

For thermal camera evaluation, the samples were kept in a refrigerator at +4°C and then were taken out and immediately placed on the heated plate at 34°C without further delay. The temperature of the samples was recorded at 10-s intervals by thermal imaging. The difference between the initial temperature measured immediately upon placement on the heating plate and the final temperature after 60 s were presented in Tables 2 and 3, for microcapsule-impregnated and nanofiber-coated knitted fabrics, respectively. According to DSC results, the best heating capacity results were obtained with Hex CA samples, and Oc TPU nanofibers could not be produced properly. Hex CA-coated samples were investigated and compared to the microcapsule-impregnated and Hex TPU-coated samples.

Thermal camera measurements did not yield significant results for samples with microcapsule applications and fabrics containing phase change materials either. This is thought to be due to their thin structures and a relatively small amount of PCM material on the single jersey fabrics. Since single jersey fabrics were too thin, when they were placed on a heating plate, the fabrics heated up very quickly and the expected results could not be observed.

According to the DSC results, no significant change was expected from the thermal camera results for the microcapsule application. Thus, this evaluation was only conducted for 200EPV-CO, 200EPV-CO/PES, and 200 EPV-CO/PAC jersey fabrics. The initial temperature of the fabrics was varied when placed on a heated plate after cooling in a refrigerator, and the final temperature of the samples was similar as shown in Figure 8. Therefore, microcapsule application did not contribute to delaying the warming of the fabrics.

From the DSC results, Hex CA nanofibers showed some heat capacity, so it was expected to obtain some sensible effect from the thermal imaging also. Thus, 40% Hex TPU and CA samples were evaluated. Although, final temperatures of 40%Hex CA-CO/PES and CO/PAC were only $\sim 1^\circ\text{C}$ lower than 40%Hex TPU-CO/PES and CO/PAC samples (Figure 9), the initial temperatures of 40%Hex CA-CO/PES and CO/PAC samples that cooled in the refrigerator were approximately $2\text{--}3^\circ\text{C}$ lower because of the synergistic effect of the Hex CA and CO/PES, CO/PAC fabrics. From these results, it can be said that Hex CA had a better effect on delaying the warming of the samples, especially for CO/PES and CO/PAC fabrics.

3.7 | Water vapor and air permeability results

Because of the best heating capacity results of Hex-CA, and the unsuccessful performance of Oc TPU nanofibers,

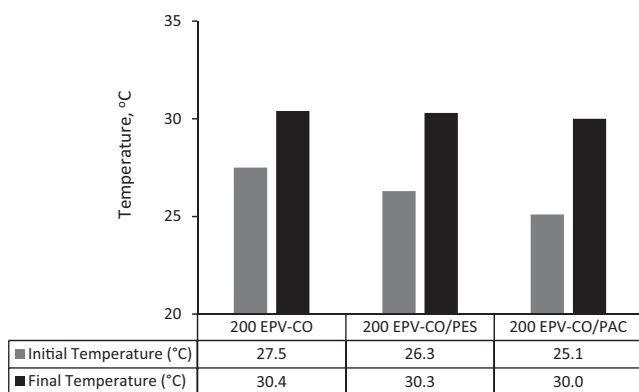


FIGURE 8 The initial and final temperature of 200 g/L microcapsule applied CO, CO/PES, and CO/PAC single jersey fabrics after 60 s by thermal imaging.

the relative water vapor permeability (%) and air permeability results were evaluated for 40%Hex TPU, and CA coated CO, CO/PES, and CO/PAC single jersey fabrics and they were compared with 200EPV applied and untreated samples. Before this comparison, microcapsule applications were compared among themselves. The results were presented in Tables 4 and 5, also figured in Figures S1 and S2.

According to the univariate analysis of variance, the microcapsule application and fabric type significantly affected the water vapor permeability ($p < 0.05$) (Table S1). According to the Tukey HSD analysis the difference between the microcapsule amount was not important but water vapor permeability was significantly lower than untreated samples (Table S2). Also, water vapor permeability results for CO, CO/PES, and CO/PAC fabrics were found to be in different subsets (Table S3). Although fabric type and microcapsule addition had a significant effect on the water permeability results, all results were high enough differing between 65% and 75%, and did not cause a commercially important difference in the ability of water vapor permeability.

Similar to the water vapor permeability results, air permeability results also were both affected from the microcapsule application and fabric type (Table S4). CO fabrics showed the lowest air permeability than CO/PAC, and CO/PES fabrics showed the highest air permeability (Table S5). However, according to Tukey HSD analysis, all three microcapsule amounts were found to be in the same subset, while untreated samples were in the other and showed higher air permeability (Table S6). The amount of microcapsule application did not significantly affect the air permeability values but these three results were lower than untreated samples. Akgunoglu et al.³¹ were also measured air permeability of microcapsule-applied polyamide fabrics as $174.5\text{ L/m}^2/\text{s}$. Microcapsule application reduced the air permeability of their fabric by

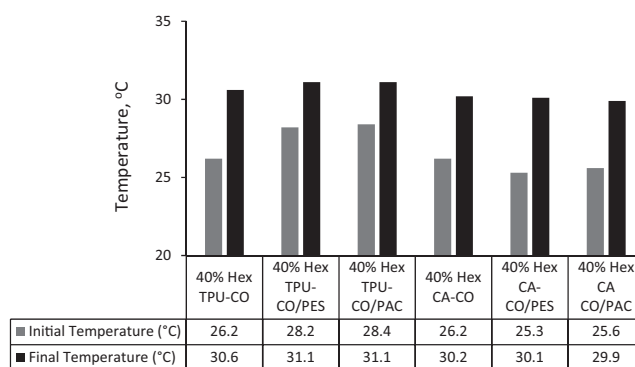


FIGURE 9 Initial and final temperature of 40%Hex TPU and CA nanofibers coated CO, CO/PES, and CO/PAC jersey fabrics after 60 s by thermal camera evaluation.

TABLE 4 Relative water permeability and air permeability of untreated and microcapsule applied CO, CO/PES, and CO/PAC fabrics.

Sample	Relative water vapor permeability (%) \pm SD	Air permeability (L/m ² /s) \pm SD
Untreated CO	65.30 \pm 1.05	345.0 \pm 8.0
Untreated CO/PES	72.20 \pm 0.30	571.0 \pm 16.8
Untreated CO/PAC	66.75 \pm 0.75	416.5 \pm 12.5
100 g/L EPV-CO	63.70 \pm 0.10	276.0 \pm 17.0
150 g/L EPV-CO	65.35 \pm 0.85	256.5 \pm 11.5
200 g/L EPV-CO	63.70 \pm 1.90	261.5 \pm 1.5
100 g/L EPV-CO/PES	71.20 \pm 0.10	394.0 \pm 15.0
150 g/L EPV-CO/PES	69.25 \pm 0.65	413.0 \pm 9.0
200 g/L EPV-CO/PES	69.25 \pm 0.75	393.5 \pm 11.5
100 g/L EPV-CO/PAC	68.30 \pm 1.00	345.5 \pm 9.50
150 g/L EPV-CO/PAC	65.30 \pm 0.10	353.0 \pm 5.0
200 g/L EPV-CO/PAC	67.45 \pm 1.05	358.0 \pm 14.0

TABLE 5 Relative water permeability (%) and air permeability of untreated and 40%Hex TPU and CA nanofiber coated CO, CO/PES, and CO/PAC jersey fabric.

Sample	Relative water vapor permeability (%) \pm SD	Air permeability (L/m ² /s) \pm SD
%40 Hex TPU-CO	67.05 \pm 0.35	3.4 \pm 0.10
%40 Hex TPU-CO/PES	70.85 \pm 1.35	6.9 \pm 0.68
%40 Hex TPU-CO/PAC	52.40 \pm 0.90	2.2 \pm 0.28
%40 Hex CA-CO	65.75 \pm 0.55	188.5 \pm 15.50
%40 Hex CA-CO/PES	67.35 \pm 2.15	297.5 \pm 6.50
%40 Hex CA CO/PAC	40.20 \pm 2.80	21.7 \pm 8.10

approximately half. Nejman et al.⁵ showed the results of air permeability for all modified fabrics were lower than the unmodified fabric, almost four times for printed and twice for padded and coated fabric.

Relative water vapor permeability and air permeability of 40%Hex-TPU and 40%Hex-CA coatings were given in Table 3. According to the univariate analysis of variance, nanofiber and fabric type had a significant effect on both the relative water vapor and air permeability (Table S7). 40%Hex-CA coated fabrics had the lowest water vapor permeability, while untreated samples had the highest (Table S8). Regarding the fabric type CO/PES fabrics showed the highest water vapor permeability, while CO/PAC fabrics showed the lowest (Table S9).

In case of air permeability results, nanofiber coating and fabric type had a significant effect on air permeability (Table S10). 40%Hex-TPU nanofibers significantly limited the air permeability of all three fabric types, and the mean result was 4.2 L/m²/s. 40%Hex-CA also decreased the air permeability to the mean of 169.2 L/m²/s, significantly lower than mean of untreated (444.2 L/m²/s) and 200EPV (337.7 L/m²/s) samples (Table S11). On the other hand, this decrease was not as large as in Hex-TPU. In the case of fabric type, the air permeability of both coated and microcapsule-applied CO/PES fabrics was higher than CO and CO/PAC fabrics (Table S12).

When we also compare the air and water vapor permeability of nanofiber coating by splitting the fabric types by One-Way ANOVA analysis (Table S13–S18), especially for CO/PAC fabrics nanofiber coating had an insignificant effect on relative water vapor permeability results. 40%Hex-CA, and 40%Hex-TPU results were also significantly different from each other, and they were lower than both untreated and 200EPV samples. For CO/PES and CO fabrics, there were some statistically significant differences, but these differences were not commercially such important, they were close and enough high for thermal comfort properties.

On the other hand, 40%Hex-TPU nanofiber coating significantly reduced the air permeability results. However, as it is indicated by the SEM results, successful Hex-CA nanofiber could not be achieved, and coating was also uneven. Due to this uneven coating, the air permeability results of 40%Hex CA-CO and CO/PES were high and different from those of the 40%Hex CA-CO/PAC fabrics. The 40%Hex-TPU nanofiber coated samples exhibited lowest air permeability, almost entirely preventing air passing from the fabrics. The 40%Hex-CA coated fabrics partially allowed the airflow but significantly less than both 200 EPV and untreated samples indicating that they can also contribute to thermoregulation behavior by blocking the airflow through the fabrics.

4 | CONCLUSION

By loading PCMs into nanofibers, the thermoregulation behavior of the traditional single jersey fabrics could be enhanced to some extent depending on the amount of PCM added. The main advantage of PCM-integrated nanofiber coating is without losing any water vapor permeability, it is possible to reduce or limit the air permeability which will help thermal comfort properties, especially in windy conditions. It was seen that, according to DSC results, PCM-integrated CA coating had better heat storage capacity than TPU nanofibers and microcapsule-applied fabrics. Although final temperatures of 40%Hex CA-CO/

PES and CO/PAC were only $\sim 1^\circ\text{C}$ lower than 40%Hex TPU-CO/PES and CO/PAC jersey fabrics, the initial temperatures of 40%Hex CA-CO/PES and CO/PAC jersey fabrics that cooled in the refrigerator were approximately $2\text{--}3^\circ\text{C}$ lower because of the synergistic effect of the Hex-CA and CO/PES, CO/PAC fabrics. In the case of air permeability results, 40%Hex TPU nanofibers significantly limited the air permeability of all three fabric types and the mean result was $4.2\text{ L/m}^2/\text{s}$ with commercially acceptable water vapor permeability (63.43%). Although PCM-loaded CA coating may not block air passage as effectively as TPU nanofibers if they would be produced much longer coating time with proper coating, they would provide better air-blocking capability along with good heat storage properties better than PCM-TPU nanofiber coated and microcapsule applied fabrics with acceptable water vapor permeability. In the continuation of this study, the use of core-shell electrospinning of CA nanofibers was planned to be investigated.

ACKNOWLEDGMENTS

The author acknowledges the Pamukkale University Research Foundation Project for the financial support (Project No: 2022HZDP010).

CONFLICT OF INTEREST STATEMENT

The authors declare that they have no known competing financial interests or personal relationships that could have appeared to influence the work reported in this paper.

DATA AVAILABILITY STATEMENT

All data generated or analyzed during this study are included in this published article.

ORCID

Çiğdem Akduman  <https://orcid.org/0000-0002-6379-6697>

Nida Oğlakcioğlu  <https://orcid.org/0000-0002-5085-7606>

Ahmet Çay  <https://orcid.org/0000-0002-5370-1463>

REFERENCES

- Shin Y, Yoo DI, Son K. Development of thermoregulating textile materials with microencapsulated phase change materials (PCM) IV. Performance properties and hand of fabrics treated with PCM microcapsules. *J Appl Polym Sci*. 2005;97(3):910-915.
- Sarier N, Onder E. Organic phase change materials and their textile applications: an overview. *Thermochim Acta*. 2012;540:7-60.
- Bashiri-Rezaie A, Montazer M. Thermal energy storage and management applications through engineered fibrous material. *Engineered Polymeric Fibrous Materials*. Woodhead Publishing; 2021:277-306.
- Tözüm M, Aksoy SA. Investigation of heat storage and comfort-related properties of the heat storing microcapsule incorporated fabrics. *J Nat Appl Sci Suleyman Demirel University*. 2014;18(2):37-44.
- Nejman A, Cieślak M, Gajdzicki B, Goetzendorf-Grabowska B, Karaszewska A. Methods of PCM microcapsules application and the thermal properties of modified knitted fabric. *Thermochim Acta*. 2014;589:158-163.
- Pervez MN, Khan A, Khan IA. Investigation on the thermoregulating fabric by using phase change material for modern textile practical application. *Am J Polym Sci Eng*. 2015;3(1):90-99.
- Song Q, Li Y, Xing J, Hu JY, Marcus Y. Thermal stability of composite phase change material microcapsules incorporated with silver nano-particles. *Polymer*. 2007;48(11):3317-3323.
- Pause B. Development of heat and cold insulating membrane structures with phase change material. *J Coat Fabr*. 1995;25(1):59-68.
- Mäkinen M. Introduction to phase change materials. *Intelligent Textiles and Clothing*. Woodhead Publishing in Textiles; 2006:21-33.
- Van Do C, Nguyen TTT, Park JS. Fabrication of polyethylene glycol/polyvinylidene fluoride core/shell nanofibers via melt electrospinning and their characteristics. *Sol Energy Mater sol Cells*. 2012;104:131-139.
- Paroutoglou E, Fojan P, Gurevich L, Hultmark G, Afshari A. Thermal analysis of organic and nanoencapsulated electrospun phase change materials. *Energies*. 2021;14(4):1-16.
- Haghighat F, Hosseini Ravandi SA, Nasr Esfahany M, Valipouri A. A comprehensive study on optimizing and thermoregulating properties of core-shell fibrous structures through coaxial electrospinning. *J Mater Sci*. 2018;53(6):4665-4682.
- Salimian S, Montazer M, Rashidi AS, Soleimani N, Bashiri Rezaie A. PCM nanofibrous composites based on PEG/PVA incorporated by TiO_2/Ag nanoparticles for thermal energy management. *J Appl Polym Sci*. 2021;138(46):51357.
- Çay A, Kumbasar EPA, Akduman Ç. Effects of solvent mixtures on the morphology of electrospun thermoplastic polyurethane nanofibres. *Tekst Konfeksiyon*. 2015;25(1):38-46.
- Nicosia A, Keppler T, Müller FA, et al. Cellulose acetate nanofiber electrospun on nylon substrate as novel composite matrix for efficient, heat-resistant, air filters. *Chem Eng Sci*. 2016;153:284-294.
- Ma Z, Kotaki M, Ramakrishna S. Electrospun cellulose nanofiber as affinity membrane. *J Memb Sci*. 2005;265:115-123.
- Luo Y, Wang S, Shen M, et al. Carbon nanotube-incorporated multilayered cellulose acetate nanofibers for tissue engineering applications. *Carbohydr Polym*. 2013;91:419-427.
- Liu X, Lin T, Gao Y, et al. Antimicrobial electrospun nanofibers of cellulose acetate and polyester urethane composite for wound dressing. *J Biomed Mater Res Part B Appl Biomater*. 2012;100:1556-1565.
- Hu L, Yan XW, Li Q, Zhang XJ, Shan D. Br-PADAP embedded in cellulose acetate electrospun nanofibers: colorimetric sensor strips for visual uranyl recognition. *J Hazard Mater*. 2017;329:205-210.
- Zhou W. Studies of electrospun cellulose acetate nanofibrous membranes. *Open Mater Sci J*. 2011;5:51-55.
- Omollo E, Zhang C, Mwasiagi JI, Ncube S. Electrospinning cellulose acetate nanofibers and a study of their possible use in high-efficiency filtration. *J Ind Text*. 2016;45:716-729.

22. Mondal S. Phase change materials for smart textiles—an overview. *Appl Therm Eng.* 2008;28(11–12):1536-1550.
23. Boguslawska-Baczek M, Hes L. Effective water vapour permeability of wet wool fabric and blended fabrics. *Fibres Text East Eur.* 2013;21(1):67-71.
24. Vadicherla T, Saravanan D. Thermal comfort properties of single Jersey fabrics made from recycled polyester and cotton blended yarns. *Indian J Fibre Text Res.* 2017;42(3):318-324.
25. Hes L. Permetest Manual, SENSORA. Accessed 31 March 2023. <http://www.sensora.eu/PermetestManual09.pdf>
26. Patanaik A, Anandjiwala RD. Modelling nonwovens using artificial neural networks. *Soft Computing in Textile Engineering.* Vol 246–267. Woodhead Publishing in Textiles; 2011.
27. Çetiner S, Belten MR. Investigation of thermoregulation properties of cotton fabrics treated with different phase change materials. *KSU J Eng Sci.* 2017;20(4):116-124.
28. McCann JT, Marquez M, Xia Y. Melt coaxial electrospinning: a versatile method for the encapsulation of solid materials and fabrication of phase change nanofibers. *Nano Lett.* 2006;6(12):2868-2872.
29. Wang N, Chen H, Lin L, et al. Multicomponent phase change microfibers prepared by temperature control multifluidic electrospinning. *Macromol Rapid Commun.* 2010;31(18):1622-1627.
30. Sun SX, Xie R, Wang XX, et al. Fabrication of nanofibers with phase-change core and hydrophobic shell, via coaxial electrospinning using nontoxic solvent. *J Mater Sci.* 2015;50:5729-5738.
31. Akgünoğlu B, Özkayalar S, Kaplan S, Aksoy SA. Comfort performances of microcapsule-applied functional socks including phase change material. *J Text Eng.* 2018;25(111):225-233.

SUPPORTING INFORMATION

Additional supporting information can be found online in the Supporting Information section at the end of this article.

How to cite this article: Akduman Ç, Oğlakcioğlu N, Çay A. Enhanced thermoregulation performance of knitted fabrics using phase change material incorporated thermoplastic polyurethane and cellulose acetate nanofibers. *Polym Eng Sci.* 2024;1-15. doi:10.1002/pen.26921